

# Feedback control of ultra-high-Q microcavities: application to micro-Raman lasers and micro-parametric oscillators

Tal Carmon, Tobias J. Kippenberg, Lan Yang, Hosein Rokhsari, Sean Spillane, and Kerry J. Vahala

*Department of Applied Physics, California Institute of Technology, Pasadena, California 91125*  
[yahala@caltech.edu](mailto:yahala@caltech.edu)

**Abstract:** We demonstrate locking of an on-chip, high-Q toroidal-cavity to a pump laser using two, distinct methods: coupled power stabilization and wavelength locking of pump laser to the microcavity. In addition to improvements in operation of previously demonstrated micro-Raman and micro-OPO lasers, these techniques have enabled observation of a continuous, cascaded nonlinear process in which photons generated by optical parametric oscillations (OPO) function as a pump for Raman lasing. Dynamical behavior of the feedback control systems is also shown including the interplay between the control loop and the thermal nonlinearity. The demonstrated stabilization loop is essential for studying generation of nonclassical states using a microcavity optical parametric oscillator.

©2005 Optical Society of America.

**OCIS codes:** (140.4780) Optical resonators; (190.5650) Raman effect; (190.4410) Nonlinear optics, parametric processes; (140.6810) Thermal effects.

---

## References and Links

1. V. B. Braginsky, M. L. Gorodetsky, and V. S. Ilchenko, "Quality-Factor and Nonlinear Properties of Optical Whispering-Gallery Modes," *Phys. Lett. A* **137** (7-8), 393-397 (1989).
2. V. S. Ilchenko, M. L. Gorodetsky, X. S. Yao et al., "Microtorus: a high-finesse microcavity with whispering-gallery modes," *Opt. Lett.* **26** (5), 256-258 (2001).
3. D. K. Armani, T. J. Kippenberg, S. M. Spillane et al., "Ultra-high-Q toroid microcavity on a chip," *Nature* **421** (6926), 925-928 (2003).
4. A. J. Campillo, J. D. Eversole, and H. B. Lin, "Cavity Quantum Electrodynamics Enhancement of Stimulated-Emission in Microdroplets," *Phys. Rev. Lett.* **67** (4), 437-440 (1991).
5. F. Treussart, J. Hare, L. Collot et al., "Quantized Atom-Field Force at the Surface of a Microsphere," *Opt. Lett.* **19** (20), 1651-1653 (1994).
6. D. W. Vernooy, A. Furusawa, N. P. Georgiades et al., "Cavity QED with high-Q whispering gallery modes," *Phys. Rev. A* **57** (4), R2293-R2296 (1998).
7. F. Vollmer, D. Braun, A. Libchaber et al., "Protein detection by optical shift of a resonant microcavity," *Appl. Phys. Lett.* **80** (21), 4057-4059 (2002).
8. S. L. McCall, A. F. J. Levi, R. E. Slusher et al., "Whispering-Gallery Mode Microdisk Lasers," *Appl. Phys. Lett.* **60** (3), 289-291 (1992).
9. V. Sandoghdar, F. Treussart, J. Hare et al., "Very low threshold whispering-gallery-mode microsphere laser," *Phys. Rev. A* **54** (3), R1777-R1780 (1996).
10. L. Yang, D. K. Armani, and K. J. Vahala, "Fiber-coupled erbium microlasers on a chip," *Appl. Phys. Lett.* **83** (5), 825-826 (2003).
11. T. J. Kippenberg, S. M. Spillane, D. K. Armani et al., "Ultralow-threshold microcavity Raman laser on a microelectronic chip," *Opt. Lett.* **29** (11), 1224-1226 (2004).
12. S. M. Spillane, T. J. Kippenberg, and K. J. Vahala, "Ultralow-threshold Raman laser using a spherical dielectric microcavity," *Nature* **415** (6872), 621-623 (2002).
13. T. J. Kippenberg, S. M. Spillane, and K. J. Vahala, "Kerr-nonlinear optical parametric oscillation in an ultrahigh-Q toroid microcavity," *Phys Rev Lett* **93** (8), - (2004).
14. Tal Carmon, H. Rokhsari, L. Yang, T. J. Kippenberg and K. J. Vahala, "Temporal behavior of radiation-pressure-induced vibrations of an optical micro-cavity phonon mode." Accepted for publication in *Phys Rev Lett*.
15. K. J. Vahala, "Optical microcavities," *Nature* **424** (6950), 839-846 (2003).

16. M. L. Gorodetsky and I. S. Grudinin, "Fundamental thermal fluctuations in microspheres," *J. Opt. Soc. Am. B* **21** (4), 697-705 (2004).
17. J. C. Knight, G. Cheung, F. Jacques et al., "Phase-matched excitation of whispering-gallery-mode resonances by a fiber taper," *Opt. Lett.* **22** (15), 1129-1131 (1997).
18. R. V. Pound, "Electronic Frequency Stabilization of Microwave Oscillators," *Rev. Sci. Instrum* **17** (11), 490-505 (1946).
19. R. W. P. Drever, J. L. Hall, F. V. Kowalski et al., "Laser Phase and Frequency Stabilization Using an Optical-Resonator," *Appl. Phys. B-Photo.* **31** (2), 97-105 (1983).
20. A. Abramovici, W. E. Althouse, R. W. P. Drever et al., "Ligo - the Laser-Interferometer-Gravitational-Wave-Observatory," *Science* **256** (5055), 325-333 (1992).
21. G. C. Bjorklund, M. D. Levenson, W. Lenth et al., "Frequency-Modulation (Fm) Spectroscopy - Theory of Lineshapes and Signal-to-Noise Analysis," *Appl. Phys. B-Photo.* **32** (3), 145-152 (1983).
22. P. Grangier, R. E. Slusher, B. Yurke et al., "Squeezed-Light Enhanced Polarization Interferometer," *Phys. Rev. Lett.* **59** (19), 2153-2156 (1987).
23. M. A. Persaud, J. M. Tolchard, and A. I. Ferguson, "Efficient Generation of Picosecond Pulses at 243nm," *Ieee J. Quantum Elect.* **26** (7), 1253-1258 (1990).
24. K. An, J. J. Childs, R. R. Dasari et al., "Microlaser - a Laser with One-Atom in an Optical-Resonator," *Phys. Rev. Lett.* **73** (25), 3375-3378 (1994).
25. A. Mugino, T. Tamamoto, T. Omatsu et al., "High sensitive detection of trace gases using optical heterodyne method with a high finesse intra-cavity resonator," *Opt. Rev.* **3** (4), 243-250 (1996).
26. T. Carmon, L. Yang, and K. J. Vahala, "Dynamical thermal behavior and thermal self-stability of microcavities," *Opt. Express* **12** (20), 4742-4750 (2004), <http://www.opticsexpress.org/abstract.cfm?URI=OPEX-12-20-4742>
27. V. S. Ilchenko and M. L. Gorodetsky, "Thermal nonlinear effects in optical whispering gallery microresonators," *Laser. Phys.* **2**, 1004-1009 (1992).
28. R. H. Stolen, J. P. Gordon, W. J. Tomlinson et al., "Raman Response Function of Silica-Core Fibers," *J. Opt. Soc. Am. B* **6** (6), 1159-1166 (1989).

---

## 1. Introduction

Surface tension induced microcavities such as microspheres [1] and microtoroids [2,3] possess ultra-high-Q (UHQ) factors making them suitable for studies of cavity quantum electrodynamics (CQED)[4, 5, 6], sensing [7], ultralow threshold lasers [8,9,10] Raman lasers [11, 12] parametric oscillators [13], radiation-pressure-induced vibrations [14] as well as for study of other nonlinear optical phenomena [15]. Generally, the combination of high Q and small mode volume improves key figures of merit in each of these applications [4-15]. In the case of nonlinear optical phenomena, microcavities make it possible to achieve enormous circulating optical powers in microscale mode volumes (on the order of  $GW/cm^2$ ). For example, 100 *Watts* of circulating power within a  $3\lambda^2$  cross section is attainable with only 1 *mWatt* coupled pump power (in surface-tension induced silica microcavities having Q factors in excess of 100 million). Nevertheless, these same desirable features of high-Q microresonators make them susceptible to noise. Specifically, their ultra-high quality factor implies an exceedingly narrow spectral linewidth so that maintaining proper alignment of pump wavelength and microcavity resonance (for efficient power coupling) can be challenging. Furthermore, the small size of the cavity also causes an increase in thermal fluctuations [16]. To address these problems, we demonstrate here a stabilization loop to lock together the pump and the microcavity resonance in an ultra-high-Q microtoroid system that is optically coupled to a fiber optic taper waveguide [17]. The resulting feedback control system enables stable operation for an unlimited duration.

In the past, Pound-Drever actively-stabilized, microwave oscillators [18], optical cavities and lasers [19] have been applied in interferometric gravity-wave detection [18,20 ], precision laser spectroscopy [21], generation of squeezed-light [22], generation of pico-second pulses [23], one atom lasers [24], heterodyne detection [25] and other applications. We therefore believe that the stable operation of ultra-high-Q microcavities, presented here, is an important enabling step in expanding the applications of UHQ cavities. In what follows, two methods of locking will be presented:

(i) Pound-Drever locking: In this method, the deviation of the pump wavelength with the cavity resonance wavelength is a feedback parameter. A typical application for such a system

is locking the pump wavelength to the center of the cavity resonance in order to achieve maximum loading of the cavity; this scheme is useful when maximal power, stable wavelength and fast feedback-control response are needed. (ii) Power locking: In this method, the deviation of absorbed pump power from a set point value is used as the feedback parameter. Power locking is valuable when steady power operation is required or when it is desirable to scan the setpoint power for data taking (e.g., measuring the L-L curve of an optically pumped laser).

## 2. Wavelength stabilized locking.

In this scheme, we first measure the deviation between the wavelengths of the pump and the cavity resonance by using the Pound-Drever method [18,19]. This method possesses high-speed reaction as it responds to the phase (rather than the frequency) [19]. We feed this error as an input to the control loop in order to stabilize the wavelength deviation between the pump and the cavity resonance. As the measured error is a function of the deviation between the wavelengths of the pump and the cavity resonance, the system will compensate for cavity-induced perturbations as well as for pump-induced perturbations. A schematic of the experimental setup is provided in Fig. 1(a). Before closing the feedback control loop, we analyze our system by measuring the Pound-Drever error signal (Fig. 1(b), bottom red trace) during a pump wavelength scan (Fig. 1(b), top-green trace) while simultaneously monitoring the cavity transmission (Fig. 1(b), middle-blue trace). Using the measured transmission, both the resonant wavelength (Fig. 1(b), top-blue) and temperature of the mode volume are calculated using a heat transfer equation as described in [26]. It is evident in Fig. 1(b) that transmission profile is a broaden triangle during the up wavelength scan (0-16 *ms*). During the down wavelength scan (16-32 *ms*) the transmission function is narrowed. The reason for this behavior is that during the upscan, the cavity is heated when pump wavelength approaches resonance and consequently the pump and the cavity resonance are traveling together (the resonance is pushed along by the sweeping pump). During the down wavelength scan, however, the sweeping pump and the resonance of the heated cavity propagate in opposing directions. As a result, the transmission line becomes narrower. This effect is generally referred to as the hysteretic wavelength response and is caused by the combined effect of thermal change of refractive index and thermal expansion of cavity [27, 26].

The measured error is consistent with the calculated, cavity, resonance wavelength as in all places where the cavity, resonance wavelength is smaller than pump wavelength the measured error is negative while in all places where the cavity resonance wavelength is larger than the pump wavelength the measured error is positive. In particular, the measured error shows that during the up-scan, the pump literally pushes the cavity resonance to longer wavelengths (see area with green background in Fig. 1(b) top) until the cavity has drifted to its maximum resonance wavelength. At this point, the resonance is rapidly lost (Fig. 1(b),  $t = 16ms$ ) as the temperature and resonance wavelength return to their equilibrium values.

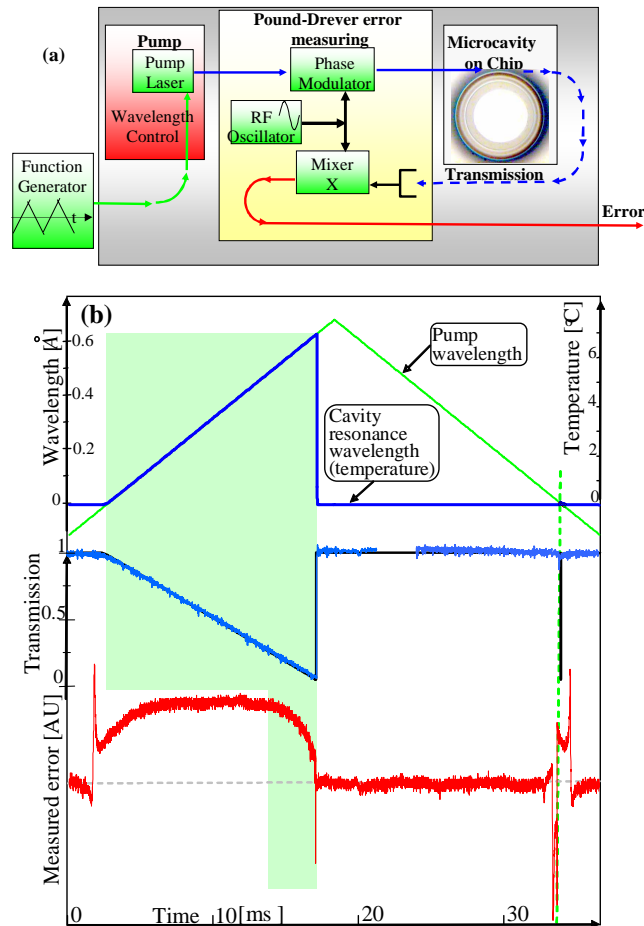


Fig. 1. (a) Pound-Drever error measurement system. (b) Parameters measured and calculated during scan of pump wavelength: Upper panel: pump wavelength (green trace), calculated cavity resonance wavelength (blue trace) and mode-volume temperature shift (blue trace, right ordinates). Middle panel: measured and calculated transmission (blue, and black respectively). Bottom panel: measured Pound-Drever error signal (red). The experimental parameters are:  $Q=2 \cdot 10^7$ ,  $\lambda_0 = 1545\text{nm}$ , pump power of  $P = 1.8\text{mW}$  and local oscillator RF frequency of 300  $\text{MHz}$ . Tunable diode laser (New Focus, Velocity) was used as a pump. Pump linewidth is 300kHz which is  $\sim 300$  times narrower than cavity linewidth.

Figure 2(a) shows the experimental setup, when the feedback control loop is closed (by feeding the error signal into a PID circuit with a controllable set point). When the control loop is closed (and the error set point is set to zero), the cavity transmission is locked to its minimum value, and the error signal is measured to be close to the setpoint value and at the same time does not change appreciably in time. The correction signal, however, exhibits large changes (comparable to hundreds of cavity widths), as it corrects large (but usually low frequency) shifts in the resonance wavelength (relative to the pump wavelength) caused, for example, by changes in room temperature, or by variation in the coupling condition to the cavity. As the measured correction amplitude can obtain values that correspond to swings in wavelength of several cavity bandwidths, it is clear that cavity locking would be lost without the active control loop.

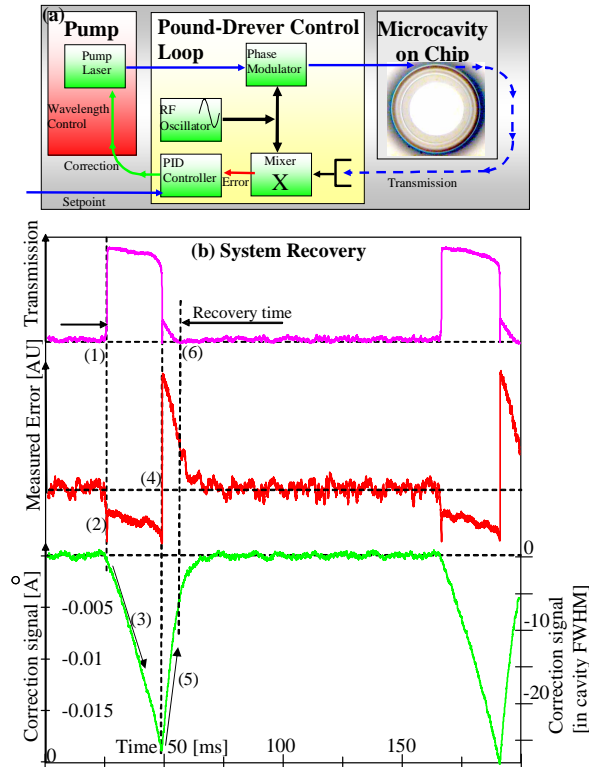


Fig. 2. Wavelength locking system incorporating Pound-Drever assembly. (a) Experimental setup. (b) System recovers from perturbation in the regime of thermal instability. The measured- transmission (upper panel), error (middle panel) and applied correction (lower panel) versus time are presented. Parameters are as in Fig. 1. Controller Integration time is 50 ms. Repeating the same experiment with faster (slower) integration time reveals faster (slower) relock events.

In order to demonstrate this locking method in the presence of perturbations, the system was intentionally pushed into a known unstable-zone (pump wavelength is slightly larger than the cavity resonance wavelength) by adjustment of the error setpoint. As noted in ref [26] this wavelength arrangement is inherently unstable because of thermal-induced instabilities. Furthermore, for illustrative purposes, the feedback control parameters were intentionally adjusted so that the feedback system would temporally lose wavelength lock.

Within the unstable regime, the loss of lock occurs at random times; the average rate of which can vary from once every minute to once every 10 ms depending upon how deeply into the unstable zone the system resides. Other important factors affecting this rate are the controller gain, integration time and the strength of noise sources perturbing the system. Obviously, loss of lock occurs when the needed correction for the noise is not supplied on time by the controller. We will now describe in Fig. 2(b) the interplay between the Pound-Drever control system, the thermal response and the optical response of the system. Figure 2(b) shows the measured-transmission (upper panel), error (middle panel) and applied correction (lower panel) versus time. When the lock is lost (time point 1) the cavity temperature (and linked resonance wavelength) rapidly decrease as pump power is no longer absorbed by the cavity. The measured error almost immediately responds (time point 2) and a strong correction signal (generated by the controller) is sent to the pump, so that the pump wavelength begins to chase (time point 3) the escaping resonance. The pump then catches the resonance and over-runs it slightly (time point 4). Next, the pump changes its propagation direction (time point 5) and ultimately lock is re-established (time point 6). After a while, a new, similar event occurs. We present this second, observed relock event in order to convince

the reader that lock recovery unfolds in an identical fashion for each such event. While here we have intentionally taken the system out of balance only to demonstrate the correction mechanism in action; we emphasize that when the controller gain is large enough and the controller integration time is short enough the controller can supply the proper timely correction and maintain lock of the pump over an unlimited duration.

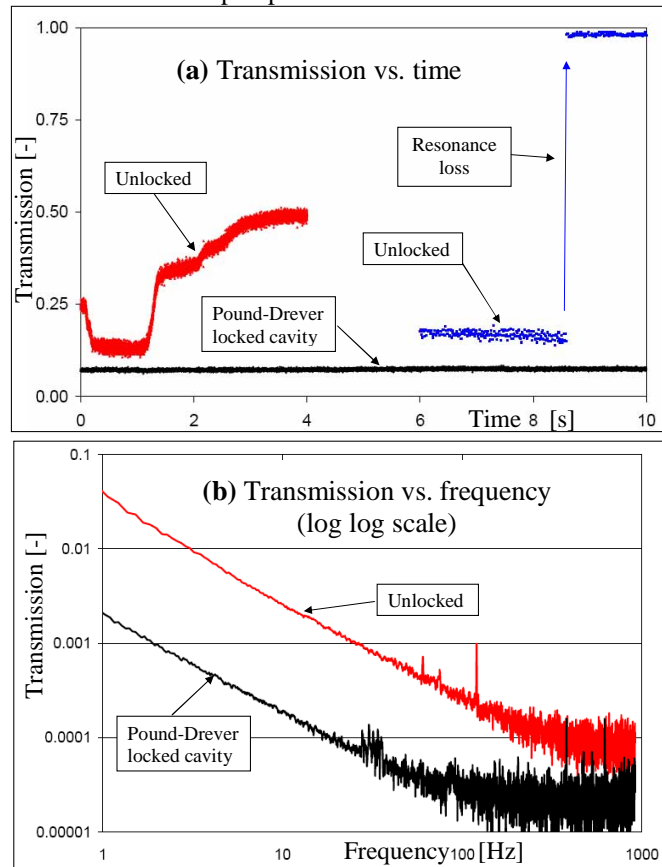


Fig. 3. (a) Cavity transmission versus time showing Pound-Drever locked cavity (black) in comparison with unlocked cavity (red and blue). Transmission of the unlocked system fluctuates (red) when pump wavelength and cavity resonance drift relative to each other. Coupling to resonance is lost (blue) when pump wavelength exceeds the thermally drifted cavity resonance. (b) Spectral analysis of locked and unlocked transmission data. The wavelength locking system incorporating Pound-Drever assembly is shown in Fig. 2(a). Integration time of the PID controller is  $20\text{ms}$ ; cavity optical quality is  $Q = 10^7$ , pump power is  $200\mu\text{W}$ .

Such a continuous lock is demonstrated in Fig. 3(a) (black), wherein the locked cavity was kept in resonance as long as the feedback system was operating. The unlocked cavity, on the other hand, exhibits transmission fluctuations as shown by the red and blue traces in Fig. 3(a). Spectral analysis of these cases is presented in Fig. 3(b) and shows an overall reduction of the fluctuation spectrum upon locking.

To conclude this section, the Pound-Drever method is useful to lock the pump to the center of the cavity absorption line. We have also demonstrated that since the error signal is valid in a zone much wider than the cavity lineshape and the reaction time is fast, it is possible for the system to overcome very large perturbations. In the example presented here (Fig. 2), the pump had to traverse more than 25 resonance widths in order to find the resonance and recover lock. In the continuous operation regime (Fig. 3), corrections were able to compensate drifts of more than 500 resonance widths.

### 3. Power stabilized locking

In this section the power coupled into the cavity is the stabilized parameter. This mode of operation is particularly useful in characterization of phenomena or devices requiring a controllable optical pump power (e.g., measuring the L-L curve of an optically-pumped laser). The Pound Drever error is not a proper reference for such a power scan since the regime in which this error is a singled valued function is very narrow (see in Fig. 1(b) the region wherein the Pound Drever error has a green background). Fortunately, another signal, the thermally modified transmission function is singled valued and a nearly linear function of the pump-resonance deviation when the pump wavelength is lower than the resonator wavelength (see transmission in Fig. 1(b) for green background). The origin of the triangular shaped (thermally modified) transmission function is addressed above. The transmission signal is also easily measured and its (singled-valued) linear behavior extends all the way from nearly-zero cavity-loading to maximal cavity-loading. As illustrated in Fig. 4(a), this transmission function will be used here as an input to the PID controller in order to make a power scan in which coupled power is stabilized.

Power stabilized locking is used here to demonstrate the cascading of parametric and Raman phenomena under controlled-pump excitation. For this demonstration, the setpoint for the power coupling into the microcavity is varied between 0 and 4 mw in steps of  $\sim 0.1 \text{ mW}$ . At each setpoint value, a spectral measurement is performed before continuing to the next setpoint. The measured spectra as a function of the coupled power are summarized in Fig. 4(b). In these spectra, the two side lobes at 1472 and 1626 nm are parametric oscillation induced by the 1545 nm pump. These idler and signal waves are the first to appear (simultaneously) and they obey  $1/\lambda_{idler} + 1/\lambda_{signal} = 2/\lambda_{pump}$ . As blue photons carry more energy than red ones, the slope of the idler power versus pump power is initially larger than the corresponding signal slope (see Fig. 4(c) inset). However, at 1.7 mW of pump power, the idler slope becomes flat (is clamped). This clamping behavior is a direct result of the idler functioning as a pump wave for Raman laser action. In particular, the onset of Raman lasing is accompanied by gain clamping, which, in this case, also clamps the idler power. In addition, Raman peaks loci here is in a region where gain is maximal when being pumped by the 1472 nm idler, for Raman gain in silica see [28]. Raman spectral peaks are noted in Fig. 4(b). In the inset of Fig. 4(c) the idler power clamping at the Raman lasing threshold is apparent. Curiously, the asymmetric clamp of one of the OPO side bands does not affect the other sideband. It is also noted here that the peaks in Fig. 3(b) are separated by the free spectral range of the test resonator.

The total nonlinearly generated optical power versus launch power is plotted in Fig. 4(c) (main panel). It follows a square root dependence on the launched pump power ( $p$ ), i.e., proportional to  $\sqrt{(p/p_{th})-1}$  where  $p_{th}$  is the threshold power. This behavior (as noted in [13]) reflects the clamping of the circulating pump-wave power within the resonator for above threshold operation.

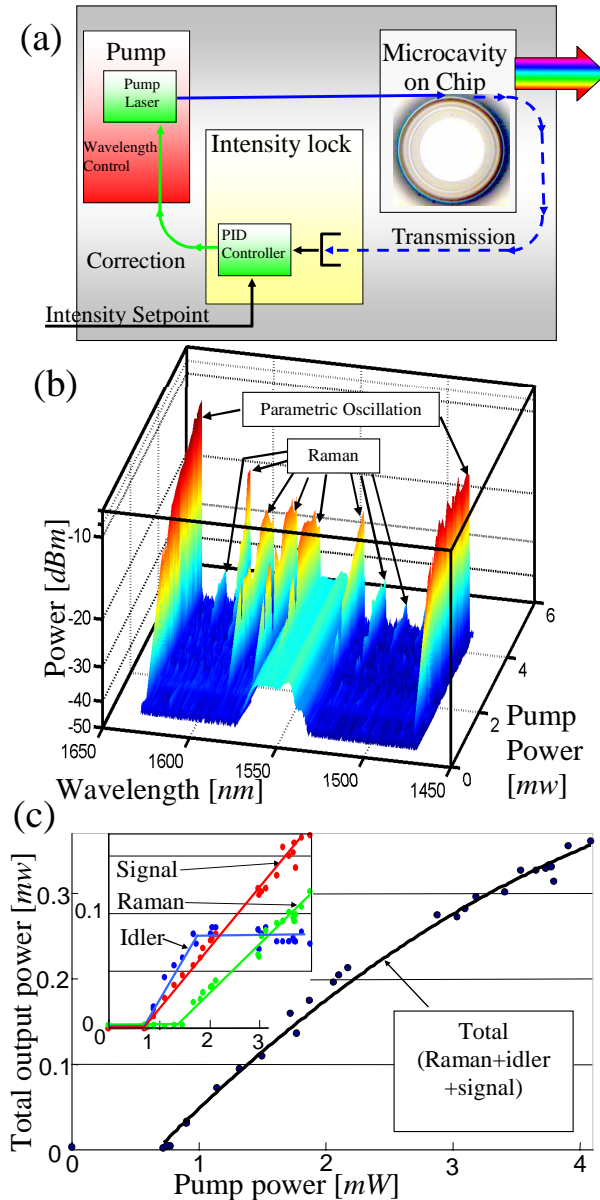


Fig. 4. Power locked cavity: (a) Experimental system, (b) parametric oscillation and Raman laser spectra as a function of the coupled power. (c) L-L curve for the total output power of the combined effect (Raman peaks + parametric oscillation's signal + idler). Line here is a fit to model. Inset: Similar L-L curves but for Raman, parametric oscillation signal, and parametric oscillation idler separately. Lines here are a guide to the eye..

To conclude this section, we have demonstrated power-stabilized parametric oscillation which stimulates Raman lasing. The locking system was observed to maintain power stability as it overcomes fluctuations caused by various sources of noise. The large separation between idler and signal presented here (154 nm) together with their stable operation make them attractive for quantum-optical correlation measurement as in such measurements low noise separation of idler, signal and pump over long periods of stable operation is required.

#### **4. Conclusions**

In this work, we have presented two methods for stabilization of ultra-high-Q microcavities. The Pound-Drever method was demonstrated and its performance analyzed as a means for wavelength-locking a pump wave to a microcavity. The effect of thermal-induced cavity drift was included in this study. In a second method, the coupled optical power was used as the feedback control parameter. This system allowed us to demonstrate a cascaded nonlinear optical process in which Raman lasing is stimulated by the idler sideband of optical parametric oscillations. To the best of our knowledge this is the first time that an optical parametric oscillation has been shown to continuously pump another nonlinear phenomenon (in our case Raman lasing). Since optical devices in general must operate continuously in the presence of various kinds of perturbations and over a large range of operation temperatures, we believe that most applications of microcavities (in laboratory as well as in industry) will require stabilization systems such as those presented here. More specifically, we believe that the stabilized microcavity OPO will be essential for quantum-optical measurements. We also expect this stabilization system to extend the capabilities of the on-chip lasers, sensors, and many other resonator-based devices.

#### **Acknowledgments**

We kindly thank Lee center for advance networking, and DARPA for their support.